Low Dielectric Constant Polyimides Derived from Novel 1,6-Bis[4-(4-aminophenoxy)phenyl]diamantane

Yaw-Terng Chern*

Institute of Chemical Engineering, National Taiwan University of Science and Technology, Taipei, Taiwan 106, Republic of China

Received June 24, 1997; Revised Manuscript Received February 13, 1998

ABSTRACT: This work reports the synthesis and characterization of diamantane-based polyimides obtained from 1,6-bis[4-(4-aminophenoxy)phenyl]diamantane and various aromatic tetracarboxylic dianhydrides. This novel polyimide exhibits a low dielectric constant (2.56−2.78), low moisture absorption (<0.292%), good solubility, and high number-average molecular weights (M_n: 3.7×10^4 to 12.8×10^4). This kind of diamantane-based polyimide can form a tough and transparent film after cyclodehydration. The films have tensile strengths of 74.4−118.2 MPa, elongations to break of 5.2−24.3%, and initial moduli of 1.9−2.2 GPa. Dynamic mechanical analysis (DMA) reveals that there is subglass relaxation above 300 °C for structures **7a**, **7d**, and **7g**, which is unusual for most of the typical polyimides. This type of novel diamantane-based polyimide is very promising for electronic applications due to its good mechanical properties, good thermal stability, low dielectric constant, and low moisture absorption.

Introduction

Diamantane is a cycloaliphatic-cage hydrocarbon containing an "extended-cage" adamantane structure.[1,2] Although diamantane has been investigated for many years, only a few examples of the polymers based on diamantane are known.[3−6] Previously, the 1,4-, 4,9- and 1,6-diethynyldiamantanes were polymerized to yield clear thermoset resins that degraded between 518 and 525 °C in air or helium.[3] In that work, colorless diamantane-based polybenzazoles were prepared via the established polyphosphoric acid polycondensation technique.[4] In addition, polycules based on diamantane have found specific applications in building dendritic materials.[5] Our recent work indicated that incorporating diamantyl units into polyamides, polyesters, and poly(amide−imide)s allowed these polymers to have good thermal stabilities, high glass transition temperatures, and good retention of storage moduli above their glass transition temperatures.[6] Regarding the incorporation of diamantane into the polyimide, only a few examples of the polyimides have been reported by us.[6f] However, polyimide films based on 1,6-diamantyl units have not been successfully prepared.[6f] Thus, the physical properties of diamantane-based polyimides (except for thermal stability) have not been reported.

Among various alternatives, carbon-based polymers with low dielectric constants (or low *K*) have received considerable attention as the dielectric materials in multilevel interconnect of integrated circuits for quarter micron technology and beyond in order to get high speed performance.[7] The major advantages of carbon-based low *K* materials used in this application are their excellent gap-filling capability and their ability to achieve a dielectric constant below 3.0. However, there are still some concerns for these materials, which are the thermal stability, the moisture pickup, the film forming capability (i.e., the precursor solubility and the molecular weight control after polymerization), their mechanical properties, their bonding strength to other interfaces, their plasma resistance during dry etching, and their solvent resistance during the wet cleaning step.

To achieve those requirements, trifluoromethyl or other perfluoroalkyl polymers have been proposed.[8−13] For instance, the highly fluorinated polyimides have dielectric constants of approximately 2.5.[8,9] Fluorinated polyaryl ethers based on decafluorobiphenyl exhibit a thermal stability comparable to that polyimides, approximately 10−40 times lower moisture absorption, dielectric constants in the mid-twos, and good retention of the storage modulus above the glass transition temperatures.[12] In addition, an alternative to push dielectric constants even lower are the closed-cell organic and/or inorganic polymeric foams, i.e., materials with significant void volumes.[14] However, preparing the homogeneous pores on the tens of nanometer size scale is relatively difficult. This work presents another approach: a diamantane-based polyimide. Diamantane is a fully aliphatic hydrocarbon, subsequently leading to high hydrophobicity and low polarity. Moreover, the diamantane cage might have a large void volume. Thus, we expect that diamantane-based polyimides to exhibit low moisture absorption and low dielectric constant.

The aim for this work is to prepare polyimides that have low dielectric constants and good environmental stability, especially materials that do not absorb moisture. Herein, we successfully synthesize new polyimides involving 1,6-bis[4-(4-aminophenoxy)phenyl)diamantane (**4**) by polycondensation with aromatic dianhydrides **5**, as shown in Scheme 2. In addition, the dielectric constants, moisture absorptions, coefficients of thermal expansion (CTE), solubilities, dynamic mechanical properties, and thermal properties of polyimides are also reported.

Experimental Section

Materials. Pyromellitic dianhydride (**5a**), 4,4′-carbonyldiphthalic anhydride (**5b**), 4,4′-oxydiphthalic anhydride (**5c**), 4,4′-hexafluoroisopropylidenediphthalic anhydride (**5d**), and 3,3′,4,4′-biphenyltetracarboxylic dianhydride (**5g**) were purified by sublimation. *N*-Methyl-2-pyrrolidone (NMP) and *m*-cresol were purified by distillation under reduced pressure over calcium hydride and stored over 4 Å molecular sieves. According to a previous method, 1,6-dibromodiamantane (**1**) was synthesized from norbornadiene in four steps.[6]

S0024-9297(97)00930-3 CCC: $15.00
Published on Web 08/08/1998

Scheme 1

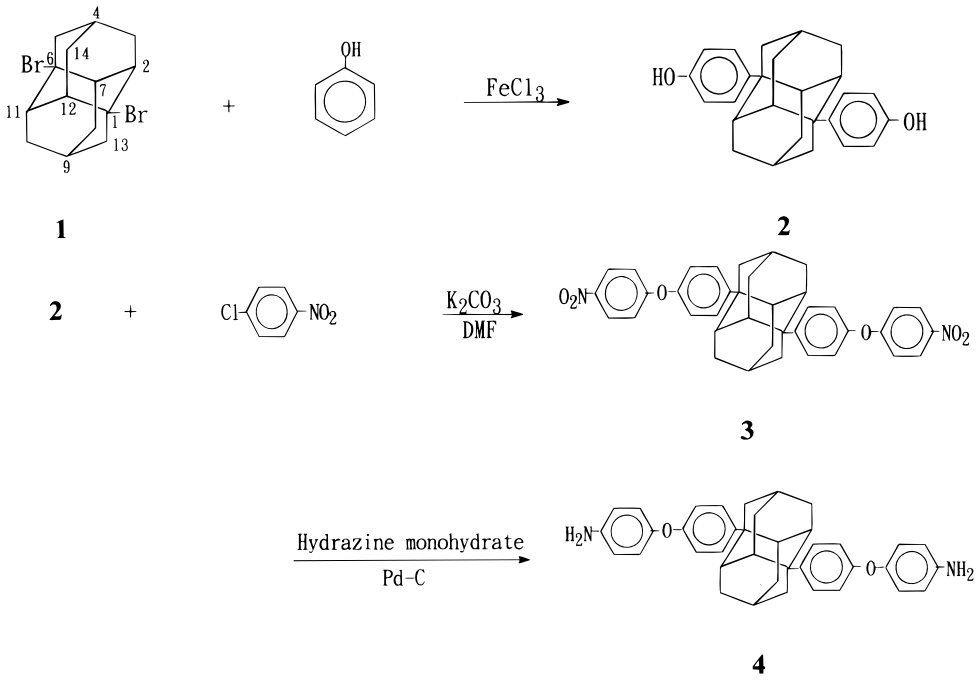

1 **2** **3** **4**

Scheme 2

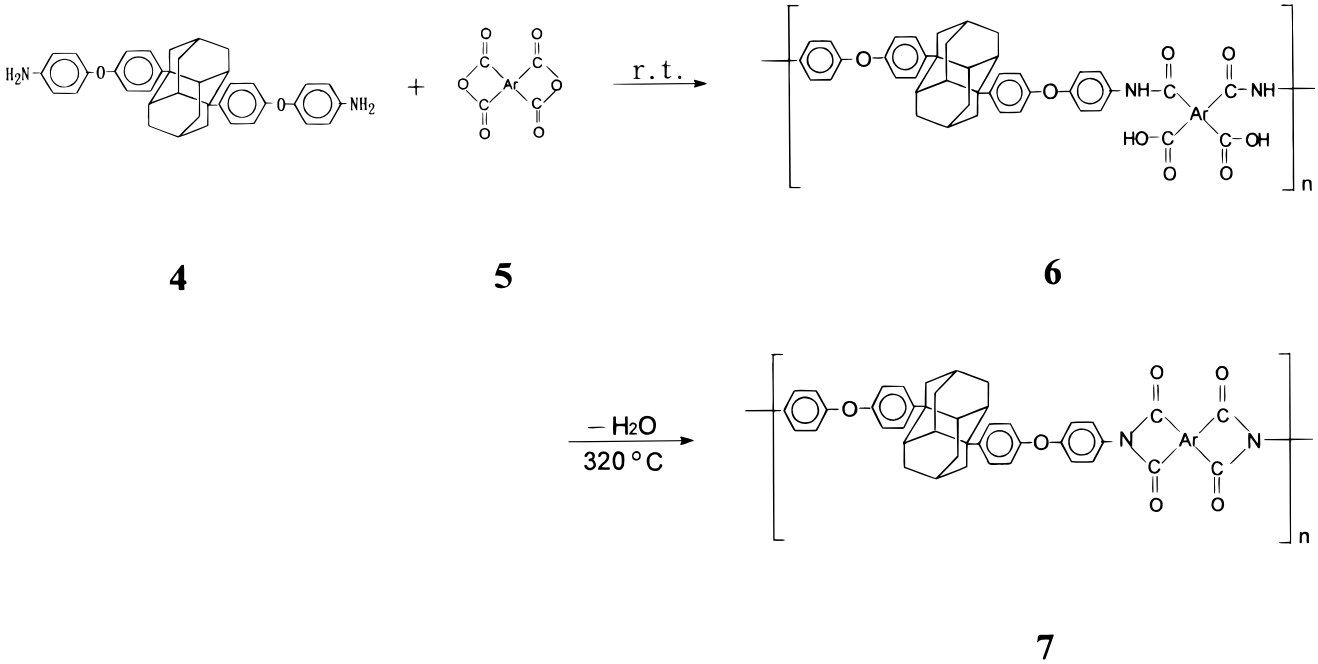

4 **5** **6** **7**

Ar: (a), (b), (c), (d), (e), (f), (g)

Herein, three steps were employed to synthesize 1,4-bis-(3,4-dicarboxyphenoxy)benzene dianhydride (**5f**) and bis[4-(3,4-dicarboxyphenoxy)phenyl] ether dianhydride (**5e**) by previous methods[15,16] from hydroquinone and 4,4′-dihydroxydiphenyl ether, respectively. The corresponding bisphenols reacted with 4-nitrophthalodinitrile in anhydrous dimethyl sulfoxide in the presence of potassium carbonate as an acid acceptor to generate bis(ether dinitrile)s which, subsequently, were then hydrolyzed to bis(ether diacid)s and dehydrated to bis(ether anhydride)s: **5e** (mp 238−240 °C, lit.[15] 238−239 °C); **5f** (mp 263−265 °C, lit.[15] 265−266 °C).

Synthesis of 1,6-Bis(4-hydroxyphenyl)diamantane (2). A mixture of 3.00 g (8.68 mmol) of 1,6-dibromodiamantane, 6 g of phenol and 0.500 g (3.08 mmol) of iron(III) chloride was stirred and heated at gentle reflux for 10 h. The reaction mixture was filtered and washed with methanol, and the precipitated solid was then crystallized from *N*,*N*-dimethylformamide (DMF) to afford 2.01 g (62.2%) of **2**: mp 358−360

°C; IR (KBr) 3285, 3076, 2890, 2867, 1647, 1546 cm^{-1}; MS (EI) *m*/*z* 372 (M^+,100), 187 (10). Anal. Calcd for $C_{26}H_{28}O_2$: C, 83.87; H, 7.53. Found: C, 83.62; H, 7.45. Crystal data: $C_{32}H_{42}N_2O_4$, colorless crystal, 0.05 × 0.20 × 0.50 mm, monoclinic $P2_1/c$ with a = 14.696(5) Å, b = 6.431(3) Å, c = 15.145(6) Å, β = 108.46(3)° with D_c = 1.269 g cm^{-3} for Z = 2, V = 1357.6(9) $Å^3$, T = 298 K, λ = 0.7107 Å, μ = 1.048 cm^{-1}, $F(000)$ = 560, intensity variation < 2%.

Synthesis of 1,6-Bis[4-(4-nitrophenoxy)phenyl]diamantane (3). A mixture of **2** (1.00 g, 2.69 mmol), *p*-chloronitrobenzene (0.938 g, 5.95 mmol), potassium carbonate (0.830 g, 6.00 mmol), and 50 mL of dry *N*,*N*-dimethylacetamide (DMAc) was refluxed at 160 °C for 12 h under nitrogen. The reaction mixture was allowed to cool to room temperature and then poured into distilled water. The precipitate was collected by filtration and recrystallized from DMAc to afford 1.26 g (76.3%) of pale yellow crystals: mp 335.5 °C (measured by DSC); IR (KBr) 3069, 2890, 2865, 1540, 1494, 1342 cm^{-1}; MS (EI) *m*/*z* 614 (M^+, 100), 228 (52). Anal. Calcd for $C_{38}H_{34}N_2O_6$: C, 74.27; H, 5.54; N, 4.56. Found: C, 74.03; H, 5.46; N, 4.48.

Synthesis of 1,6-Bis[4-(4-aminophenoxy)phenyl]diamantane (4). A 150 mL, three-necked, round-bottomed flask was charged with **3** (1.00 g, 1.63 mmol), 10 mL of hydrazine monohydrate, 80 mL of ethanol, and 0.03 g of 10% palladium on carbon (Pd−C). The mixture was heated at reflux for 16 h and then filtered to remove the Pd−C, and the crude solid was recrystallized from DMAc to afford 0.831 g (92.2%) of white crystals: mp 302−304 °C; IR (KBr) 3469, 3376, 3076, 2890, 2867, 1613, 1503 cm^{-1}; MS(EI) *m*/*z* 554 (M^+, 97), 277 (100). Anal. Calcd for $C_{38}H_{38}N_2O_2$: C, 82.31; H, 6.86; N, 5.05. Found: C, 82.15; H, 6.78; N, 4.96. Crystal data; $C_{46}H_{56}N_4O_4$, very pale yellow crystal, 0.10 × 0.20 × 0.50 mm, monoclinic $P2_1/c$ with a = 20.031(4) Å, b = 6.366(3) Å, c = 15.479(5) Å, β = 98.96(3)° with D_c = 1.242 gcm^{-3} for Z = 2, V = 1949.6(11) $Å^3$, T = 298 K, λ = 0.7107 Å, μ = 0.540 cm^{-1}, $F(000)$ = 784.

Characterization. A Bio-Rad FTS-40 FTIR spectrophotometer was used to record IR spectra (KBr pellets). MS spectra were obtained by using a JEOL JMS-D300 mass spectrometer. ^1H and ^{13}C NMR spectra were recorded on a Bruker AM-300WB or AM-400 Fourier transform nuclear magnetic resonance spectrometer using tetramethylsilane (TMS) as the internal standard. A Perkin-Elmer 240C elemental analyzer was used for the elemental analysis. The X-ray crystallographic data were collected on a CAD-4 diffractometer. The analyses were carried out on a DEC Station 3500 computer using NRCC SDP software. The melting points were obtained by a standard capillary melting point apparatus. Inherent viscosities of all polymers were determined at 0.5 g/dL using an Ubbelohde viscometer. Gel permeation chromatography (GPC) on soluble polymers was performed on an Applied Biosystem at 70 °C with two PLgel 5 μm mixed-C columns in the NMP/LiBr (0.06 mol/L) solvent system. The flow rate was 0.5 mL/min, detection was by UV, and calibration was based on polystyrene standards. Qualitative solubility was determined using 0.01 g of polymer in 2 mL of solvent. A Du Pont 9900 differential scanning calorimeter and a Du Pont 9900 thermogravimetric analyzer were employed to study the transition data and thermal decomposition temperature of all the polymers. The differential scanning calorimeter (DSC) was run under a nitrogen stream at a flow rate of 30 cm^3/min and a heating rate of 20 °C/min. The thermogravimetric analysis (TG) was determined under a nitrogen flow of 50 cm^3/min. Dynamic mechanical analysis (DMA) was performed on a Du Pont 9900 thermal analyzer system. A sample 10 mm in length, 2 mm in width, and approximately 0.05 mm in thickness was used. The dynamic shear modulus was measured at a resonance mode. The wide-angle X-ray diffraction measurements were performed on a Philips PW 1730-10 X-ray diffractometer using Cu Kα radiation.

Tensile properties were determined from stress−strain curves with a Toyo Baldwin Instron UTM-III-500 with a load cell of 10 kg at a drawing speed of 5 cm/min. Measurements were performed at 28 °C with the film specimens (about 0.1 mm thick, 1.0 cm wide, and 5 cm long), and an average of at least five individual determinations was used. The in-plane, linear coefficient of thermal expansion (CTE) was obtained from a TA TMA-2940 thermomechanical analyzer (5 °C/min, from 30 to 250 °C, 10 mN). The CTE value on the temperature scale between 50 and 200 °C was recorded after an initial conditioning step (heat to 250 °C, hold 5 min, and cool). Moisture absorption measurements were made with an ultramicrobalance of Sartorius model S3D−P on thin films (~40 μm). Measurements were taken at 30 °C for 90 h at 85% relative humidity. Dielectric constants were measured by the parallel-plate capacitor method using a dielectric analyzer (TA Instruments DEA 2970) on thin films. Gold electrodes were vacuum deposited on both surfaces of dried films, followed by measuring at 25 °C in a sealed chamber at 0% relative humidity.

Polymerization. Two typical examples of polycondensation are given below.

Polymer Synthesis by the Two-Step Method. Dianhydride **5d** (0.444 g, 1.00 mmol) was added to a stirred solution of **4** (0.554 g, 1.00 mmol) in NMP (solid content 11% w/v) under N_2 and reacted at ambient temperature for 6 h. The inherent viscosity of the poly(amic acid) **6d** in NMP was 0.97 dL/g, measured at a concentration of 0.5 g/dL at 30 °C. The IR spectrum exhibited absorptions at 3345 (N−H and O−H str), and 1720, 1650 (C═O str) cm^{-1}, which were characteristic of the amic acid. The poly(amic acid) solution was then cast onto a glass plate. The poly(amic acid) **6d** was converted to polyimide **7d** by successive heating in a vacuum at 80 °C for 3 h, at 200 °C for 8 h, and, then, at 320 °C for 6 h. The inherent viscosity of **7d** was 0.69 dL/g, measured at a concentration of 0.5 g/dL in chloroform at 10 °C. The FTIR spectrum of **7d** exhibited absorptions at 1779 (asym C═O str), 1728 (sym C═O str), 1372 (C−N str), and 718 cm^{-1} (imide ring deformation), which were characteristic of the imide group.

Polymer Synthesis by the One-Step Method. Dianhydride **5d** (0.444 g, 1.00 mmol) was added to a stirred solution of **4** (0.554 g, 1.00 mmol) in *m*-cresol (solid content 5% w/v) containing 2% of isoquinoline at 25 °C in N_2 atmosphere. The solution, after being stirred for 3 h, was heated at reflux (200 °C) for 5 h. During this time, the water of imidization was allowed to distill from the reaction mixture. The *m*-cresol was continually replaced to maintain the total volume of the solution. The solution, after cooling to ambient temperature, was diluted with 10 mL of *m*-cresol and then slowly added to 500 mL of vigorously stirred ethanol. The polymer that precipitated was collected, filtered, washed with ethanol and water, and dried under reduced pressure at 150 °C for 8 h. The inherent viscosity of **7d** was 1.29 dL/g, as measured at a concentration of 0.5 g/dL in NMP at 30 °C.

Results and Discussion

Monomer Synthesis. 1,6-Bis[4-(4-aminophenoxy)-phenyl]diamantane (**4**) was synthesized from 1,6-dibromodiamantane (**1**) in three steps as shown in Scheme 1. According to Scheme 1, **1** was reacted with phenol in the presence of iron(III) chloride as a catalyst to give **2**. Reaction of bisphenol **2** with *p*-chloronitrobenzene in anhydrous DMAc in the presence of potassium carbonate as an acid acceptor gave **3**, which was hydrogenated to give monomer **4**. The high yield of **3** (76.3%) in the condensation reaction of *p*-chloronitrobenzene with the dipotassium salt of **2** can be attributed to the high nucleophilicity of **2** which results from the electron donating ability of the diamantyl group. The ^{13}C chemical shifts for compound **4** were assigned on the basis of a DEPT experiment (Figure 1A). The chemical shifts for protons in compound **4** were assigned with the aid of the 2D $^1H-^{13}C$ COSY spectrum (Figure 1B). On the individual carbon atoms (C-3, -8, -10, -14) in a rigid diamantyl ring, an equatorial proton was found to be further downfield by 0.33 ppm than the axial proton (see Table 1, compound **4**). This occurrence is

Table 1. NMR Spectral Data for Compounds 2, 3, and 4

compd	solvent	mode	proton or carbon type,[a] δ, ppm
2	DMSO-d_6[b]	^{1}H NMR (400 MHz)	1.41−1.46 (t, 8H, H-3a, -5, -8a, -10a, -13, -14a), 1.65 (brs, 2H, H-4, -9), 1.81 (d, J = 11.7 Hz, 4H, H-3e, -8e, -10e, -14e), 2.50 (brs, 4H, H-2, -7, -11, -12), 6.71 (d, J = 8.7 Hz, 4H, H-c), 7.16 (d, J = 8.7 Hz, 4H, H-b), 9.12 (s, 2H, OH)
3	$CDCl_3$	^{1}H NMR (300 MHz)	1.53−1.59 (d, J = 19.7 Hz, 8H, H-3a, -5, -8a, -10a, -13, -14a), 1.81 (brs, 2H, H-4, -9), 1.95 (d, J = 12.5 Hz, 4H, H-3e, -8e, -10e, -14e), 2.60 (brs, 4H, H-2, -7, -11, -12), 7.01−7.07 (m, 8H, H-c, -f), 7.45 (d, J = 8.8 Hz, 4H, H-b), 8.20 (d, J = 8.7 Hz, 4H, H-g)
3	$CDCl_3$	^{13}C NMR (75 MHz)	27.94 (C-4, -9), 33,25 (C-3, -8, -10, -14), 39.11 (C-2, -7, -11, -12), 41.57 (C-1, -6), 49.90 (C-5, -13), 116.96 (C-c), 120.39 (C-f), 125.93 (C-g), 127.37 (C-b), 142.44 (C-h), 146.17 (C-a), 151.89 (C-d), 163.58 (C-e)
4	DMSO-d_6	^{1}H NMR (300 MHz)	1.45 (d, J = 17.5 Hz, 8H, H-3a, -5, -8a, -10a, -13, -14a), 1.67 (brs, 2H, H-4, -9), 1.78 (d, J = 12.2 Hz, 4H, H-3e, -8e, -10e, -14e), 2.50 (brs, 4H, H-2, -7, -11, -12), 4.95 (s, 4H, NH_2), 6.57 (m, 4H, H-g), 6.75−6.81 (m, 8H, H-c, -f), 7.29 (d, J = 8.9 Hz, 4H, H-b)
4	DMSO-d_6	^{13}C NMR (75 MHz)	27.41 (C-4, -9), 32.74 (C-3, -8, -10, -14), 38.30 (C-2, -7, -11, -12), 40.58 (C-1, -6), 49.53 (C-5, -13), 114.60 (C-g), 116.25 (C-c), 120.65 (C-f), 126.44 (C-b), 141.61 (C-h), 145.27 (C-a), 145.66 (C-e), 156.23 (C-d)

[a] The atom labeling used here is the same as in Scheme 1 and Figure 1A. [b] DMSO-d_6: dimethyl sulfoxide-d_6.

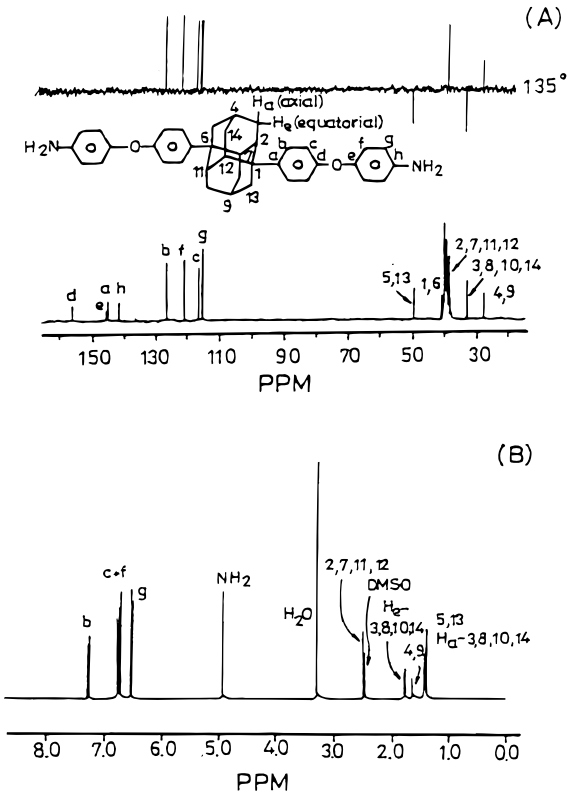

Figure 1. NMR (DMSO-d_6) spectra of **4**. (A) ^{13}C 135° DEPT and ^{13}C NMR (100 MHz); (B) ^{1}H NMR (400 MHz).

attributed to the fact that the equatorial proton is within the deshielding cone of the neighboring C−C bond. When **3** was converted into the diamine **4**, the reasonances of protons H_g shifted from 8.20 to 6.57 ppm (see Table 1). The structures of compounds **2** and **4** were also confirmed by X-ray diffraction analysis. The X-ray crystal data for **4** was acquired from a single crystal crystallized from DMAc solution. A single crystal of **2** was also obtained by slowly crystallizing it from a DMF solution. Interestingly, **4** and DMAc (molecular ratio = 1:2) formed a single-crystal complex via a hydrogen bond; **2** and DMF also formed a single-crystal complex via a hydrogen bond. Figure 2 illustrates the X-ray structure of **4**. The ^{1}H and ^{13}C NMR spectra of these new monomers showed the characteristic peaks of the assigned structures (Table 1). In addition, the elemental analysis and the IR spectra also verify these new monomers.

Synthesis of Polymers. New diamantane-based polyimides were synthesized by a conventional two-step procedure starting from **4** and aromatic tetracarboxylic dianhydrides **5** through the ring-opening polyaddition and subsequent thermal cyclodehydration (Scheme 2). Table 2 summarizes those results. The solution polymerization reaction was initially heterogeneous, but gradually homogenized as the monomers dissolved. Notably, the viscosity increased within ∼30 min of stirring at room temperature. Viscosity buildup, however, was markedly slower than for standard diamines such as 4,4′-oxydianiline. This slower buildup was probably due to the bulky and rigid diamantyl ring which increases the polymer chain's rigidity. The more rigid polymer chain implies a longer reaction time to produce the high inherent viscosity. In addition, the ring-opening polyaddition in NMP at room temperature afforded poly(amic acid)s **6** with high inherent viscosities (between 0.75 and 1.15 dL/g). The IR spectroscopy confirmed the formation of poly(amic acid)s. The characteristic absorption bands of the amic acid appeared near 3345 (N−H and O−H str), 1720 (acid, C═O str), 1650 (amide, C═O str), and 1540 cm^{-1} (N−H bending). Next, the thermal conversion to polyimides **7** was performed by successively heating the poly(amic acid)s. The soluble polyimides **7** had inherent viscosities of 0.41−1.29 dL/g. According to GPC data, medium and high molecular weights were usually attainable (Table 2). In fact, all M_w/M_n's were lower than those of the commercial materials, which may be due to the somewhat low reactivity of **4** containing a rigid and bulky diamantyl unit. Table 2 also indicates that the molecular weights of the polyimides **7** prepared by the one-step method exceeded those of the polyimides **7** prepared by a two-step method. This finding closely resembles that in previous literature.[17] IR spectroscopy confirmed the formation of polyimides **7**. The characteristic absorption bands of the imide ring appeared near 1780 (asym C═O str), 1720 (sym C═O str), 1390 (C−N str), and 745 cm^{-1} (imide ring deformation). In addition, NMR spectra also confirmed the polyimide **7d**, as shown in Figure 3. In the proton spectrum, *m* and *n* were assigned while assuming that the *n* proton ortho to the C═O had shifted farther downfield. Also, the *m* proton signal was broadened through interaction with the nearby CF_3 groups and, possibly, by unresolved meta coupling with the *k* proton. Herein, the ^{13}C NMR spectrum of **7d** was assigned using a combination of DEPT, 2D ^{1}H−^{13}C COSY, and the results for carbon

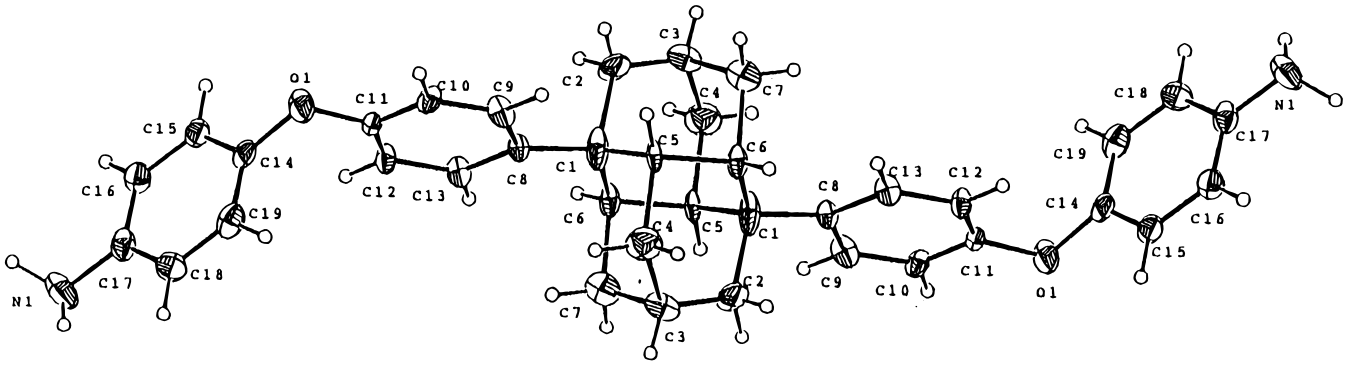

Figure 2. X-ray structure of **4**.

Table 2. Inherent Viscosities and GPC Molecular Weights of Poly(amic acid)s and Soluble Polyimides

	poly (amic acid)s	polyimides		
dianhydride	η_{inh} (dL/g)[a]	M_n[e] $\times 10^{-4}$	M_w/M_n	η_{inh} (dL/g)[a]
5a	1.15	*f*		
5b	0.75			
5c	0.90	5.6	1.8	0.41[b]
5d	0.97	3.7	1.8	0.69[b]
5e	0.89	5.9	1.9	0.64[c]
5f	0.97			0.56[c]
5g	1.06			
5d[d]		12.8	1.8	1.29
5e[d]		11.5	1.6	1.21

[a] Measured in NMP at 0.5 g/dL at 30 °C. [b] Measured in chloroform at 0.5 g/dL at 10 °C. [c] Measured in *o*-chlorophenol at 0.5 g/dL at 30 °C. [d] Prepared in m-cresol containing 2% isoquinoline at 200 °C. [e] By GPC (relative to polystyrene). [f] Could not be measured.

assignments in compound **3**. In the carbon spectrum, the *i* and *j* assignments were made while assuming that the *i* carbon para to the $C(CF_3)_2(Ph)$ had shifted farther downfield. In addition, splitting of the *o* carbon absorption was observed due to long-range effects by the CF_3 fluorine. Similarly, the *p* carbon absorption was split into a quartet by the fluorine.

Characterization of Polymers. The solubilities of the polyimides were tested in various solvents. Table 3 summarizes those results. Owing to the bulky diamantyl units and flexible ether segments, the polyimides **7** were amorphous and soluble in a number of common organic solvents, e.g., chloroform, *m*-cresol, *o*-chlorophenol, or THF. Even the nonfluorinated polyimides **7c**, **7e**, and **7f** were soluble in *o*-chlorophenol, *m*-cresol, and chloroform. A comparison of the solubility of **7e** with the corresponding polyimide derived from **5e** and 4,4′-oxydianiline shows that polyimide **7e** has better solubility. We believe that, for the polymers considered herein, perhaps the bulky diamantyl units that prevent spontaneous parallel alignment of the rodlike molecules significantly weaken these forces of attraction. The hexafluoroisopropylidene-containing polyimide **7d** exhibited an excellent solubility toward the test solvent. The polyimide **7d** was soluble in *o*-chlorophenol, *m*-cresol, THF, and chloroform. However, the polyimides **7a**, **7b**, and **7g** were insoluble in the test solvent owing to their relatively rigid anhydride moieties.

Transparent and pale yellow polyimide films **7** were obtained by successively heating the corresponding poly(amic acid)s **6**. All polyimide films **7** were tough. Initially, the polyimide films **7** were structurally characterized by the wide-angle X-ray method. As Figure 4 indicates, all polyimides **7** had nearly the same

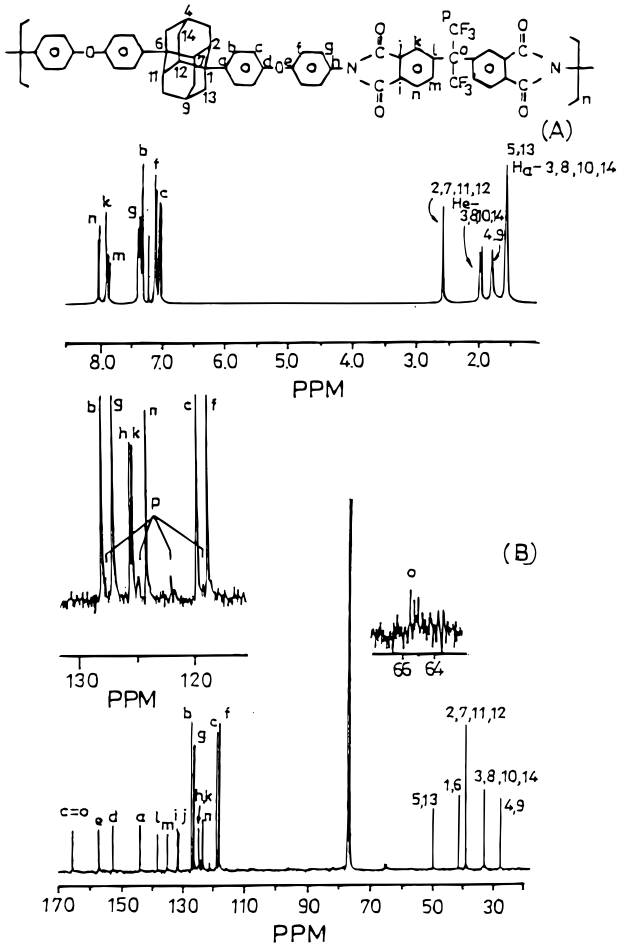

Figure 3. NMR ($CDCl_3$) spectra of polyimide **7d**: (A) ^{1}H NMR (400 MHz); (B) ^{13}C NMR (100 MHz).

amorphous patterns, with exhibited a broad peak appearing at around 15° (2θ).

Table 4 summarizes the dielectric constants, moisture absorptions, CTE, and mechanical properties. The mechanical properties were determined via an Instron machine. The mechanical properties of polyimides **7**, in general, are satisfactory. When compared to the polyimides based on the more flexible anhydride, i.e., **5c**, **5e**, and **5f**, these polyimides gave fairly high values of elongation to break. These higher elongations likely result from the more flexible nature of the backbone due to the presence of the flexible anhydrides.

The moisture absorptions of polyimides **7** are extremely small, <0.3% (Table 4), because of the water proofing effect of the fluorine atoms and diamantane elements. The absorbed moisture of polymers heavily

Table 3. Solubilities of Polyimides[a]

solvent	solubility of polymer							
	7a	**7b**	**7c**	**7d**	**7e**	**7f**	**7g**	ref[b]
o-chlorophenol	−	−	+−	+−	+	+	−	+−
m-cresol	+−	+−	+−	+	+	+−	+−	+−
chloroform	−	−	++	++	++	+	+−	−
THF	−	−	−	+	+−	+−	−	−
NMP	−	−	+−	+	+−	−	−	+−
DMAc	−	−	+−	+−	+−	+−	−	+−

[a] Solubility: ++, soluble at room temperature; +, soluble on heating at 60 °C; +−, partial soluble on heating at 60 °C; −, insoluble on heating at 60 °C. Abbreviation: NMP, *N*-methyl-2-pyrrolidone; DMAc, *N*,*N*-dimethylacetamide; THF, tetrahydrofuran. [b] An aromatic polyimide was synthesized from **5e** and 4,4′-oxydianiline in our laboratory.

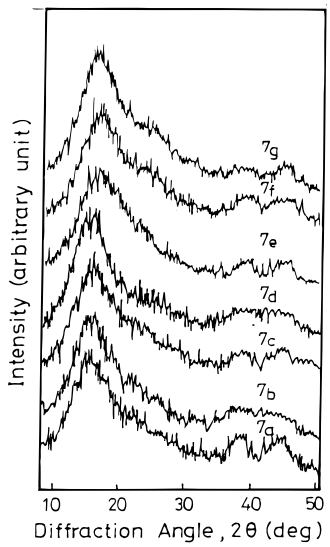

Figure 4. Wide-angle X-ray diffraction curves of polyimides.

influences their dielectric constants.[8] Table 4 also indicates that the dielectric constants of diamantane-based polyimides **7** are low, ranging from 2.56 to 2.78. Even the nonfluorinated polyimides **7** also had low dielectric constants. Such low dielectric constants result from the fact that diamantane is a fully aliphatic hydrocarbon, subsequently leading to low hydrophobicity and polarity. We speculate that this causes a "dilution" effect of the polar imide groups by the diamantyl units (on a weight basis based on polymer).

The CTEs of polyimides **7** resemble those of flexible polyimides[10] (see Table 4). This similarity is because polyimides **7** have bent ether units and bulky diamantyl units. These bent units and bulky groups loosen the films' molecular packing. In addition, producing a polyimide film from polyimide solution generally yields a lower CTE than from the corresponding poly(amic acid).[9] Herein, the polyimide films **7** using for measuring CTE were obtained by casting from the corresponding poly(amic acid). Thus, the CTEs of polyimides **7** were moderate.

Thermal analysis was performed by means of DSC, DMA, and TGA. Table 5 summarizes those results. The polyimides **7** did not decompose until 400 °C in air and nitrogen atmosphere, and their temperatures at a 5% weight loss ranged from 460 to 509 °C in air and from 505 to 529 °C in N_2 atmosphere. The influences of residual water or solvent and history of thermal annealing were occasionally observed in the initial DSC heating run. Therefore, the first heating of the samples was curtailed at 400 °C. In addition, T_g and other thermal properties were assessed according to the DSC charts of the second heating. According to Figure 5, all polyimides **7**, except **7a**, displayed typical glass transitions. The glass transition temperatures of **7** were found to be 280−365 °C. The rigid and bulky diamantyl unit increases the polymer chain's rigidity which, in turn, gives high glass transition temperatures. Polyimides containing the more flexible ether segments, i.e., **7e** and **7f**, exhibited lower T_gs. Moreover, the T_gs of polyimides **7** decreased markedly with increasing content of the ether segment.

More detailed information can be obtained from the dynamic mechanical behavior measurements taken of the films as a function of temperature. Herein, films of around 50 μm thickness were studied between 0 and 450 °C. Figure 6 depicts mechanical relaxation spectra of polyimide **7a**. On the basis of tan δ and G'' peaks, three relaxations were observed at ca. 104, 303, and >445 °C. The low-temperature transition, termed β_2 (ca. 104 °C), is a typical β relaxation for standard polyimides. This relaxation is associated with a steady decrease in G'. Such a transition has generally been attributed to the rotation or oscillations of the phenyl groups within the polyimide's diamine moiety.[18,19] The second transition, named β_1, at 303 °C, is associated with an approximately $^1/_4$ order of magnitude step decrease in G'. Small transition peaks in tan δ and G'' also appear in β_1 relaxation. Moreover, the β_1 relaxation occurs at a markedly higher temperature (at 303 °C) than typically found in most other polyimides. The actual reason for this transition still remains uncertain. We believe that the high subglass relaxation occurs in extremely rigid polyimides, as discussed below with polymers **7d** and **7g**. The temperature of this last transition from a glassy state to a rubbery plateau cannot be determined precisely from the mechanical relaxation spectra. Although the flexible ether segments were incorporated in the polyimide **7a** backbone, it had a high T_g, over 445 °C. This finding is attributed the fact that the rigid anhydride **5a** and the rigid diamantyl unit were incorporated into polyimide **7a**.

The mechanical relaxation spectra of **7d** and **7g** resemble those of **7a**. Three relaxation transitions were also observed in the polymers **7d** and **7g**, based on tan δ and G'' peaks. The low-temperature β_2 transitions of **7d** and **7g** shifted to 210 and 150 °C, respectively. Moreover, during β_2 transitions for both cases, the broad disperse peaks appeared in tan δ and G''. The high-temperature β_1 subglass transitions of **7d** and **7g** appeared at 300 and 280 °C, respectively. This relaxation is also associated with a step decrease in G'. Coburn et al. also reported that a high subglass relaxation at 300 °C occurred in the extremely rigid polyimides.[20] From the above results, we can infer that this high subglass relaxation at around 300 °C apparently occurs in the extremely rigid polyimides. The glass transitions of **7d** and **7g** appeared at very high temperatures, 375 and 386 °C, respectively.

Figure 7 illustrates the mechanical relaxation spectra of **7c**. Two relaxation transitions appeared at ca. 120 and 340 °C, based on tan δ and G'' peaks. A broad disperse β_2 peak appeared at around 120 °C in tan δ and G''; this transition is associated with a decrease in G'. The reason for such a transition resembles that of the β_2 transition of **7a**. However, the high-temperature β_1 subglass transition around 300 °C was not observed in polyimide **7c**. This finding is attributed to the fact

Table 4. Physical Properties of Polyimide Films

polymer	strength to break (MPa)	elongation to break (%)	initial modulus (GPa)	CTE (ppm/°C)	% H_2O absorption[a] 85% RH	dielectric constant (dry, 1 kHz)
7a	90.9	8.3	2.2	45.3	0.132	2.65
7b	91.5	9.1	2.0	41.6	0.292	2.78
7c	118.2	24.3	1.9	53.5	0.138	2.68
7d	74.4	5.2	2.2	44.1	0.121	2.56
7e	101.3	17.5	1.9	52.2	0.162	2.65
7f	104.9	13.8	1.9	54.8	0.173	2.64
7g	100.5	10.2	2.2	46.9	0.150	2.63

[a] Moisture absorptions of polyimide films were measured at 30 °C for 90 h.

Table 5. Thermal Properties of Polyimides

polymer	DSC[a] T_g (°C)	DMA[b] T_g (°C)	DMA[b] T_{β_1} (°C)	DMA[b] T_{β_2} (°C)	dec[c] temp (°C) in Air	dec[c] temp (°C) in N_2
7a	*d*	>445	303	104	502	525
7b	365	360		132	506	516
7c	352	340		120	463	524
7d	361	375	300	210	460	512
7e	280	283		136	481	505
7f	311	302		100	490	521
7g	358	386	280	150	509	529

[a] Glass transition temperature (T_g) measured by DSC at a heating rate of 20 °C/min in nitrogen. [b] The glass and subglass transitions measured by DMA using shear mode at a heating rate of 5 °C/min. [c] Temperature at which 5% weight loss was recorded by TG at a heating rate of 10 °C/min. [d] Not found.

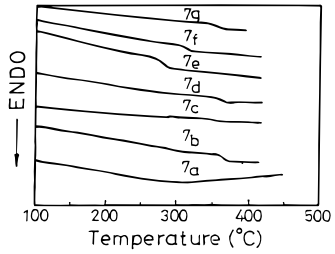

Figure 5. DSC thermograms of the studied polymers at a heating rate of 20 °C/min in nitrogen atmosphere.

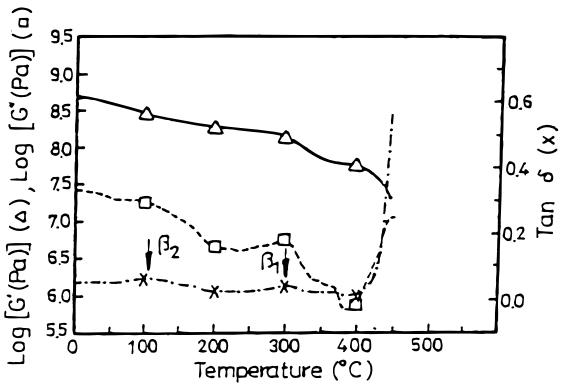

Figure 6. Dynamic mechanical analysis curves (G', shear storage modulus; G'', shear loss modulus) for **7a** at a heating rate of 5 °C/min.

that polyimide **7c** is relatively less rigid than polyimides **7a**, **7d**, and **7g**, thereby suggesting that the high subglass β_1 relaxation occurs in the extremely rigid polyimides. The glass transition of **7c** at 340 °C is associated with an approximately 2 orders of magnitude decrease in G'. The mechanical relaxation spectra of the other polyimides (**7b**, **7e**, and **7f**) resembles those of **7c**. Table 5 also summarizes the glass and β relaxation temperatures of polyimides **7**. The high-temperature β_1 subglass relaxation was not observed in the three polyimides **7b**, **7e**, and **7f**. The reason for the absence of high subglass relaxation is the same as

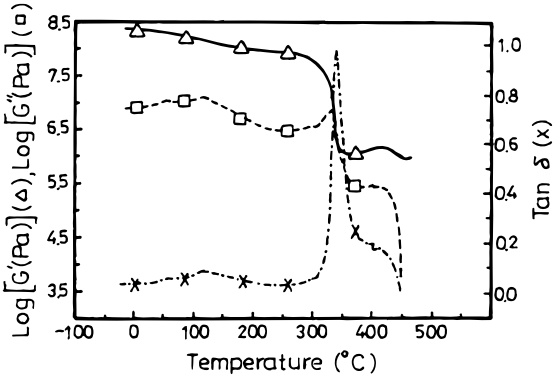

Figure 7. Dynamic mechanical analysis curves (G', shear storage modulus; G'', shear loss modulus) for **7c** at a heating rate of 5 °C/min.

polyimide **7c**. This table also indicates that as the dianhydride was varied for a given diamine the T_g roughly followed the order **5a** > **5g** > **5d** > **5b** > **5c** > **5f** > **5e** (by DMA). Although the flexible ether segments were incorporated into the polyimide **7** backbone, the T_gs of polyimides **7** exceeded 340 °C, except **7e** and **7f**. This finding is due to the fact that the rigid and bulky diamantyl units inhibited the rotation of bonds, resulting in an increasing chain stiffness. On the other hand, owing to the incorporation of relatively high content of ether segments, the T_gs of **7e** and **7f** are lower than the other polyimides **7**. In addition, the β_2 subglass relaxation temperatures of polyimides **7** vary widely. This variation suggests that interactions between different polymeric chains are essential.

The subglass relaxations in most polyimides occur over a broad range from 50 to 200 °C. Herein, the β_1 transitions (ca. 280−300 °C) of the very rigid polyimides **7a**, **7d**, and **7g** occurred at significantly higher temperatures than typically observed in polyimides. However, the β_1 transition was not observed in the relatively less rigid polyimides **7b**, **7c**, **7e**, and **7f**. Thus, high-temperature subglass relaxation apparently occurs in the extremely rigid polyimides.

Conclusions

Owing to the low hydrophobicity and polarity of the rigid and bulky diamantane, the merits of new diamantane-based polyimides are high solubilities, low dielectric constants, low moisture absorptions, and high T_gs. In addition, the diamantane unit can readily be incorporated into polyimides through the extended monomer method to obtain high molecular weight materials. This kind of diamantane-based polyimide can form tough and transparent pale yellowish films. These films display good mechanical properties and good thermal stabilities. DMA reveals that three transitions appeared in the extremely rigid polyimides **7a**, **7d**, and **7g**. The low-

temperature β_2 subglass relaxation is a typical β relaxation for standard polyimides. Another high-temperature β_1 subglass relaxation (ca. 270−300 °C) occurs at a much higher temperature than typically observed in most other polyimides. However, the β_1 transition was not observed in relatively less rigid polyimides **7b**, **7c**, **7e**, and **7f**. Thus, high subglass relaxation seems to occur in the extremely rigid polyimides. Their glass relaxation processes occur at high temperatures exceeding 340 °C, except for **7e** and **7f**. Due to the bent ether units and bulky diamantyl group, the CTEs of these films are moderate.

Acknowledgment. We are grateful to the National Science Council of the Republic of China for the support of this work.

References and Notes

(1) Olah, G. A.; Prakash, G. K. S.; Shin, J. G.; Krishnamurthy, V. V.; Mateescu, G. D.; Liang, G.; Sipos, G.; Buss, V.; Gund, T. M.; Schleyer, P. v. R. *J. Am. Chem. Soc.* **1985**, *107*, 2764.
(2) Vogel, O.; Anderson, B. C.; Simons, D. M. *Tetrahedron Lett.* **1966**, 415.
(3) Malik, A. A.; Archibald, T. G.; Baum, K. *Macromolecules* **1991**, *24*, 5266.
(4) Dang, T. D.; Archibald, T. G.; Malik, A. A.; Bonsu, F. O.; Baum, K.; Tan, L. S.; Arnold, F. E. *Polymer Prepr. (Am. Chem. Soc., Div. Polym. Chem.)* **1991**, *32* (3), 199.
(5) Chapman, O. L.; Ortiz, R. *Polymer Prepr. (Am. Chem. Soc., Div. Polym. Chem.)* **1995**, *36* (1), 739.
(6) (a) Chern, Y. T.; Wang, W. L. *Macromolecules* **1995**, *28*, 5554. (b) Chern, Y. T. *Macromolecules* **1995**, *28*, 5561. (c) Chern, Y. T.; Fang, J. S.; Kao, S. C. *J. Polym. Sci., Polym. Chem. Ed.* **1995**, *58*, 1417. (d) Chern, Y. T.; Wang, W. L. *J. Polym. Sci., Polym. Chem.* **1996**, *34*, 1501. (e) Chern, Y. T.; Chung, W. H. *Makromol. Chem. Phys.* **1996**, *197*, 1171. (f) Chern, Y. T. *J. Polym. Sci., Polym. Chem.* **1996**, *34*, 125.
(7) Tummala, R. R.; Keyes, R. W.; Grobman, W. D.; Kapin, S. *Microelectronics Packaging Handbook*; Tummala, R., Rymaszewski, E. J., Eds; Van Nostrand Reinhold: New York, 1989; Chapter 9.
(8) (a) Misra, A. C.; Tesoro, G.; Hougham, G.; Pendharkar, S. M. *Polymer* **1992**, *33*, 1078. (b) Hougham, G.; Tesoro, G.; Shaw, J. *Macromolecules* **1994**, *27*, 3642. (c) Hougham, G.; Tesoro, G.; Viehbeck, A. *Macromolecules* **1996**, *29*, 3453. (d) Hougham, G.; Tesoro, G.; Viehbeck, A.; Chapple-Sokol, J. D. *Macromolecules* **1994**, *27*, 5964.
(9) (a) Feiring, A. E.; Auman, B. C.; Wonchoba, E. R. *Macromolecules* **1993**, *26*, 2779. (b) Trofimenko, S.; Auman, B. C. *Macromolecules* **1994**, *27*, 1136.
(10) (a) Ichino, T.; Sasaki, S.; Matsuura, T.; Nishi, S. *J. Polym. Sci., Polym. Chem.* **1990**, *28*, 323. (b) Matsuura, T.; Hasuda, Y.; Nishi, S.; Yamada, N. *Macromolecules* **1991**, *24*, 5001.
(11) Mercer, F. W.; Mckenzie, M. T. *High Perform. Polym.* **1993**, *5*, 97.
(12) Irvin, J. A.; Neef, C. J.; Kane, K. M.; Cassidy, P. E.; Tullos, G.; St. Clair, A. K. *J. Polym. Sci., Polym. Chem.* **1992**, *30*, 1675.
(13) Bruma, M.; Fitch, J. W.; Cassidy, P. E. *J. Macromol. Sci. Rev. Macromol. Chem. Phys.* **1996**, *C36* (1), 119.
(14) Hrubesh, L. W.; Keene, L. E.; LaTorre, V. R. *J. Mater. Res.* **1993**, *8*, 1736.
(15) Takekoshi, T.; Kochanowski, J. E.; Manello, J. S.; Webber, M. J. *J. Polym. Sci. Polym. Chem.* **1985**, *23*, 1759.
(16) Eastmond, G. C.; Parotny, J. *Macromolecules* **1995**, *28*, 2140.
(17) Harris, F. W.; Hsu, S. L.-C. *High Perform. Polym.* **1989**, *1*, 1.
(18) Bernier, G. A.; Kline, D. E. *J. Appl. Polym. Sci.* **1968**, *12*, 593.
(19) Perena, J. M. *Angew. Makromol. Chem.* **1982**, *106*, 61.
(20) Coburn, J. C.; Soper, P. D.; Auman, B. C. *Macromolecules* **1995**, *28*, 3253.

MA970930B